International Journal of Advanced Chemistry, 14 (1) (2026) 10-15

International Journal of Advanced Chemistry

Website: www.sciencepubco.com/index.php/IJAC
https://doi.org/10.14419/qzm4wd02
Research paper

Extraction and Structural Characterization of Cellulose From Balanites Aegyptiaca Seed Shell

Alhassan Adeku Sallau *

Chemistry Advanced Research Center, SHESTCO, Abuja, Nigeria
**Corresponding author E-mail: creamysal@yahoo.co.uk*

Received: January 7, 2026, Accepted: March 18, 2026, Published: March 25, 2026

Abstract

This study explores the isolation and characterization of cellulose from Balanites aegyptiaca Seed Shell, a novel and sustainable source. Following alkaline treatment and bleaching, the extracted cellulose was analyzed using Fourier Transform Infrared Spectroscopy (FTIR), X-Ray Diffraction (XRD), Scanning Electron Microscopy (SEM), and Thermogravimetric Analysis (TGA). The results reveal the presence of characteristic functional groups: hydroxyl (-OH), methylene (-CH), and β(1→4)-glycosidic (C-O) bonds, indicative of cellulose. XRD analysis showed the existence of the 002 plane associated with cellulose with a high crystallinity index (89.28% to 63.74%) and crystal sizes (31.63 nm to 30.11 nm). SEM images revealed agglomerated cellulose fibers with smooth surfaces and varying sizes, indicating high purity. Thermal stability evaluation using TGA showed a two-stage degradation process, with the main degradation occurring between 231.51°C and 448.18°C, indicating moisture loss and carbon gasification. The results suggest that Balanites aegyptiaca seed shell is a viable cellulose source for biodegradable composites, food, and cosmetics. The high crystallinity index, crystal size, and thermal stability make the extracted cellulose suitable for these applications. This study contributes to research on sustainable materials, highlighting agricultural waste as a valuable cellulose production resource.

Keywords: *Alkaline Extraction; Balanites Aegyptiaca; Cellulose; Crystallinity Index; Crystal Size; Dehydration; Environmental Sustainability; Microcrystal.*

1. Introduction

The increasing global concerns about environmental sustainability and the implementation of new environmental regulations have driven the search for eco-friendly materials [1]. Cellulose, the most abundant biopolymer in nature, has gained significant attention due to its estimated annual production of 5 million tons [2]. The isolation of nanocellulose from waste materials has become an attractive approach, offering economic and environmental benefits. Over the past decade, research on extracting cellulose from waste has gained momentum. Agricultural waste, such as rice husk [3], green bamboo [4], plum seed shells [5], mango seed [6], corn cob, banana plant, cotton stalk, and cotton gin waste [7], pineapple [8], cassava peel [9], jackfruit peel [10], sugar bagasse [11] and Natural Areca Fiber[12], have been explored as potential sources for crystalline cellulose fibers. Various terms, including nano-whiskers, cellulose nanocrystals, mono-crystals, micro-crystals, or micro-crystallites [3] have been used to describe the crystalline cellulose obtained.
Despite the extensive research on natural fibers, Balanites aegyptiaca Seed Shell remains an underexplored source for cellulose production. Balanites aegyptiaca (L.) Delile, a perennial tree native to semiarid regions in sub-Saharan Africa, has been widely distributed in the Arabian Peninsula and South Asia [13]. Known by various vernacular names, including 'Aduwa' in Hausa and 'Tanni' in Fulani, this tree has a long lifespan of up to 100 years, with 75 years of fruiting [14]The fruit, a drupe with an epicarp, mesocarp, endocarp, and kernel, was reported to contain between 30-60% oil and 20-30% protein in the kernel [15]. The hull, comprising 85% fiber, has a cellulose composition of 60%, hemicellulose of 31%, and lignin of 9% [16].
This study aims to isolate cellulose from Balanites aegyptiaca Seed Shell using alkaline, perchlorite, and acetic acid/peroxide treatments.

2. Materials and Methods

2.1. Pretreatment of Balanites aegyptiaca seed shell samples

Balanites aegyptiaca Seed Shell samples were obtained from Katsina State, Nigeria. The seeds were cracked open, and the hull was air-dried for 48 hours. The hull was then ground using a TRAPP Animal Ration shredder hammer mill (Foliage TRF 80) and sieved through a set of five sieves with sizes ranging from 1.18 mm to 0.075 mm. Samples with particle sizes <75 µm, 75 µm, and 150 µm were utilized for the cellulose extraction and also characterized for extractives, moisture, cellulose, hemicellulose, lignin, and ash content.

2.2. Alkali treatment

Alkali treatment was performed to purify the cellulose by removing lignin and hemicellulose from the Balanites aegyptiaca Seed Shell fibers. The ground samples (10 g) were boiled in 100 mL of 1 mol/dm³ sodium hydroxide solution for 30 minutes. The mixture was cooled, filtered under vacuum, washed three times with 100 mL of distilled water, and then transferred to a beaker for the bleaching process.

2.3. Bleaching process

The bleaching process was carried out by adding 100 mL of a mixture of 10% acetic acid solution and a 2% hypochlorite solution to the washed samples from the alkaline treatment, similar to the method reported by [17]. The mixtures were refluxed for 4 hours, cooled, and filtered. The residue was washed using excess distilled water. The bleaching process was repeated twice.

2.4. Characterization of cellulose

The functional group was investigated using a Thermo Scientific Nicolet iS5 Fourier Transform Infrared (FTIR) spectroscopic equipped with the diamond attenuated total reflectance (ATR) while scanning the spectra between 400 and 4000nm wavelength. The surface morphology of cellulose structures were analyzed using a Phenom ProX Desktop SEM (10–15 kV) equipped with an EDS silicon drift detector, with samples mounted on carbon-taped aluminum stubs and imaged under [High Vacuum/Charge Reduction; the micrographs were captured at an accelerating voltage of 15 kV with magnification scales up to 1500x. Thermal stability was assessed using a PerkinElmer TGA 4000 at a heating rate of 10°C/min from 30–900°C under a nitrogen atmosphere. The crystalline phases of the cellulose materials were characterized using the PANalytical Empyrean diffractometer in a Theta/Theta goniometer configuration, with Cu as the irradiated source at both wavelengths of Kα (1.5406 Å) and Kβ (1.5444 Å) generated at 45 kV and 40 mA. Data acquisition was performed via the Gonio scan axis with a minimum step size of 0.0001° in 2theta. Purity, ash content, and moisture content were also determined using standard methods.

3. Results and Discussion

3.1. Structural functional group characterization of cellulose

The structural functional groups present in the cellulose of Balanites aegyptiaca Seed Shell are shown in Fig. 1. The broad band peaks at 3321.78, 3354.08, and 3325.64 cm^{-1} exhibited by all the cellulose size types are attributed to the O-H stretching of hydroxyl groups in the cellulose structure. According to Ogunjobi and Balogun [18], these peaks are due to intra-molecular and intermolecular hydrogen bond vibrations. While the study by Rajanna et al. [17] suggested that the peak at 3352 cm^{-1} could be linked to the presence of CH_2 groups, which also suggests the presence of intermolecular hydrogen bonding attraction between the -CH_2 groups in addition to the elongating force experienced by the CH_2 from the -OH groups present. These two observations insinuate that there is the presence of the polysaccharide aromatic ring and β-glycosidic linkage. The peaks at 2894.62, 2889.08, and 2898.48 cm^{-1} are associated with the -C-H asymmetric stretching of methylene (-CH_2) groups in cellulose [18]. Similar peak positions were reported by Liew et al. [4] and [19] for isolated cellulose obtained from biomass. Additionally, Mohd Jamil et al. [20] reported a peak at 2920 cm^{-1} corresponding to the asymmetrical stretching vibration of C-H groups in polysaccharides. A strong to weak peak observed at 2358-2359 cm^{-1} may be attributed to the presence of background CO_2, as reported by Md Salim et al. [21] and Mugesh et al. [22]. However, these peaks are not a common feature of cellulose structure.

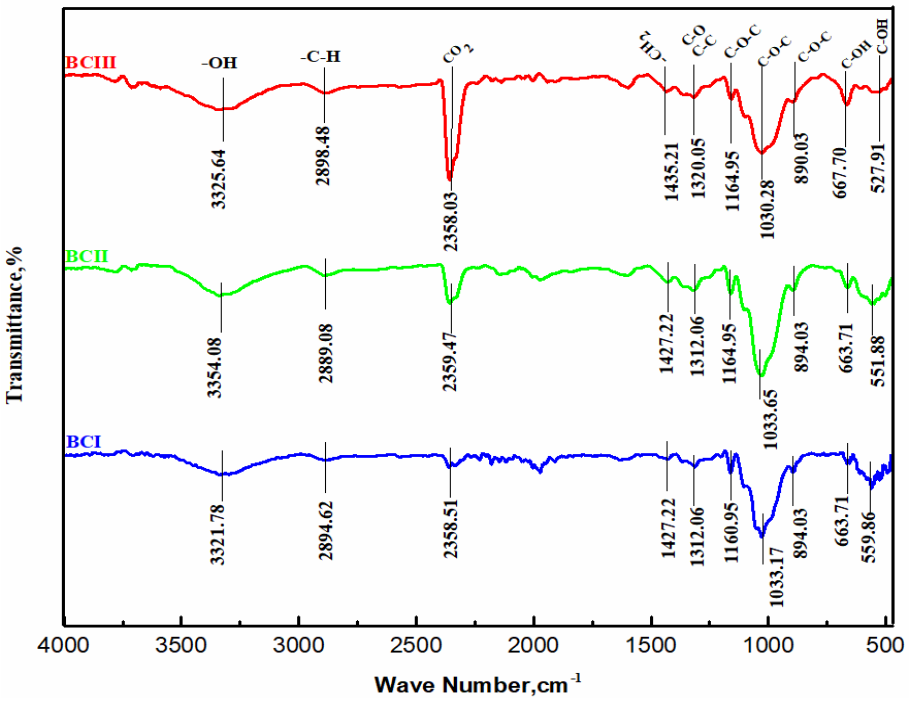

Fig. 1: FTIR Spectrum of Cellulose Extract of Balanites Aegyptiaca Seed Shell.

The peaks observed at 1322.44, 1310.87, and 1316.66 cm^{-1} are attributed to symmetric C-H bending, which is similar to the deformation vibrations of OH groups, as suggested by Coates [23]. Additionally, the peaks at 1033.17, 1033.65, and 1030.28 cm^{-1} represent the stretching of C-O bonds in C-OH of alkanols or C-O-C bonds of ether in the cellulose structure. A closer examination of the peaks obtained from the three cellulose samples reveals variations in peak intensity, particularly at the 2358.03 peak position. Notably, the cellulose sample obtained from the 150 µm particle size showed the highest intensity compared to the samples from the <75 µm and 75 µm particle sizes.

3.2. Structural crystallinity

The diffractograms of cellulose samples Fig. 2 indicated that BCI, BCII, and BCIII exhibit a hump peak at 22.6° and 34.88°, corresponding to the crystallographic planes of 200 and 004, respectively. According to Ogunjobi et al. [24] and Romruen et al. [25], these peaks are characteristic of the cellulose-I structure. The study by Cheran et al. [26] attributed the peaks observed at 2θ positions of 15.80, 22.03, 26.69, and 40.44° to cellulose and suggested that the characteristic peak at 22º, which is assigned to the 002 plane, is associated with crystallinity, while the broadening of the peak is attributed to increased amorphousity. The crystallinity index of the synthesized cellulose was calculated using the following formula:

$$CI = \frac{Area\ of\ crystalline\ peak}{Area\ crystalline\ and\ ammorphous\ peaks} \times 100$$ [24]

Accordingly, the CI values of 89.28, 77.38, and 63.74 % for the BCI, BCII, and BCIII samples, respectively was obtained. This suggested that the CI of the cellulose increases with reduced precursor size. The CI of 89.28% for the BCI was notably higher than the range of 77 to 84% reported by Mishra et al. [27], while that of BCII was within the range. This suggests that Balanites shells contain highly ordered crystalline regions that enhance mechanical strength. The values of CI obtained for BC I, II, and III were all higher than 33.1% reported for extractive free biomass (EFB) sample by Zambrano-Mite et al. [28] because the EFB has a high content of non-cellulosic components, which led to the low CI value. Similarly, Khan et al. [29] reported a crystallinity value of 63.58±5 % for cellulose from Marrubium vulgare which was higher than those of cellulose obtained from rice straw (30–55 %) reported by Oun and Rhim, [30], wheat straw (35–65 %) and cotton (30–60 %) as reported by Huntley et al., [31].

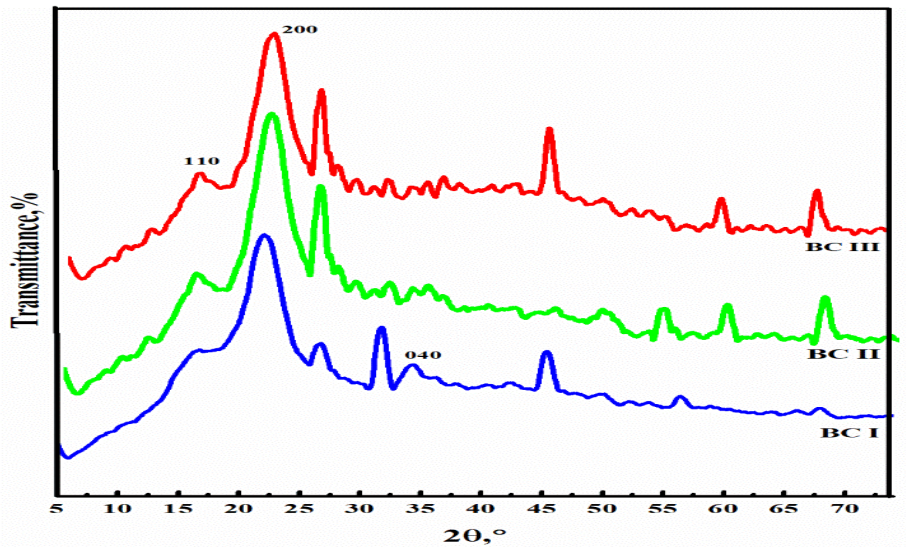

Fig. 2: X-Ray Diffractogram of Cellulose Extract of Balanites Aegyptiaca Seed Shell.

While the crystalline size of the cellulose BCIII, BCII, and BCI was found to be 31.63,30.53 and 30.11 nm, respectively, according to Scherrer's equation.

$$crystal\ size\ L = \frac{k\lambda}{\beta \cos\theta}$$ [24]

Where K is the Scherrer constant 0.94, λ is 0.15406 Å, β is the full width at half maximum (FWHM), and θ is the peak. The crystalline size was smaller compared to the size reported for cellulose obtained from Typha angustifolia, which was 308.3 µm and 280.9 µm [32]. Similarly, Khan et al. [29] reported the size of cellulose from Marrubium vulgare as 32.5 Å, which also appeared to be **much smaller** than the values obtained for BCI, BCII, and BCIII. While Sathishkumar et al. [33] reported a smaller crystal size of 10.68 nm for cellulose from the Bitter Albizia tree. This indicated that the crystallite size of cellulose can vary widely according to the source and process of extraction and purification. In addition to the cellulose peaks observed in the BCI, BCII, and BCIII XRD patterns, other developing peaks at positions of 24°, 26°, 32°and 45°, which were observed maybe attributed to possible reflection, characteristic of mineral elements linked to ash content of the cellulose.

3.3. Structural morphology

The morphological features of the cellulosic products obtained from Balanites aegyptiaca Seed Shell, as shown in Fig. 3, reveal an agglomeration arrangement of cellulose fiber filaments with networks of interconnected fibers. The fibers exhibit varying sizes, curled shapes, and relatively smooth surfaces with few visible pores. These morphological characteristics suggest that careful control of the extraction process

may enable the isolation of microfiber forms of the cellulose material. This could potentially lead to various applications, including: Reinforcing agents in biodegradable composites and gel-forming agents in food and cosmetics. This is consistent with the findings of Khenblouche et al. [34], who highlighted the potential of microfiber cellulose in various applications.

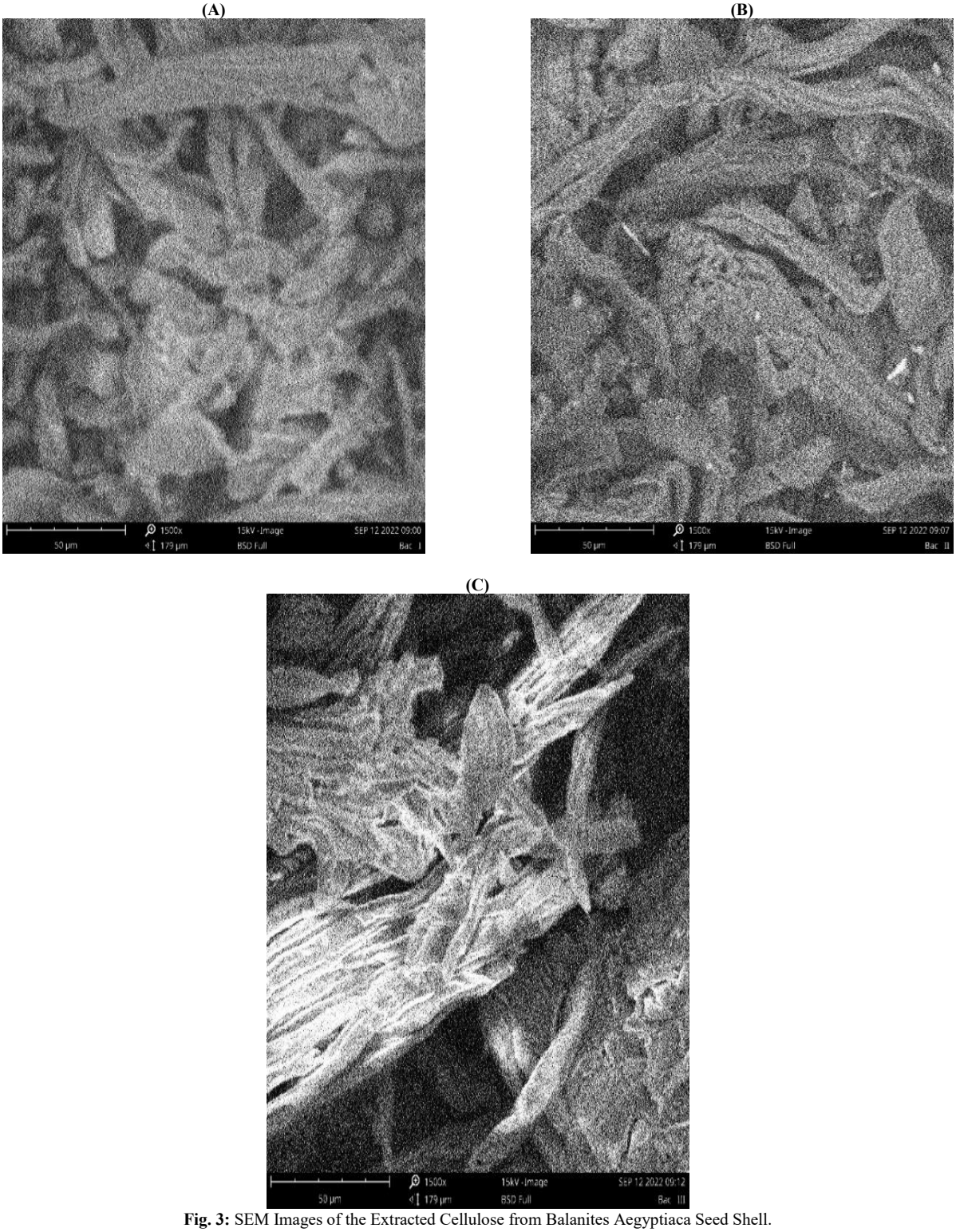

Fig. 3: SEM Images of the Extracted Cellulose from Balanites Aegyptiaca Seed Shell.

3.4. Thermal stability

The thermal behavior of the cellulosic products obtained is illustrated in Fig. 4. The thermogravimetry (TG) curves in plot (a) reveal a two-stage degradation process for the cellulose samples, consistent with the typical thermal profile expected for cellulosic materials [35]. The first stage of weight loss, ranging from 2.26% to 2.98%, occurs between 59.31°C and 200.18°C for the three cellulose samples (BCI, BCII, and BCIII). This initial weight loss is attributed to the dehydration stage, where water molecules are released from the extracted cellulose. The differential thermogravimetry (DTG) curve in Figure (b) shows that the peak volatilization of water molecules from the cellulose samples occurs at approximately 100°C.

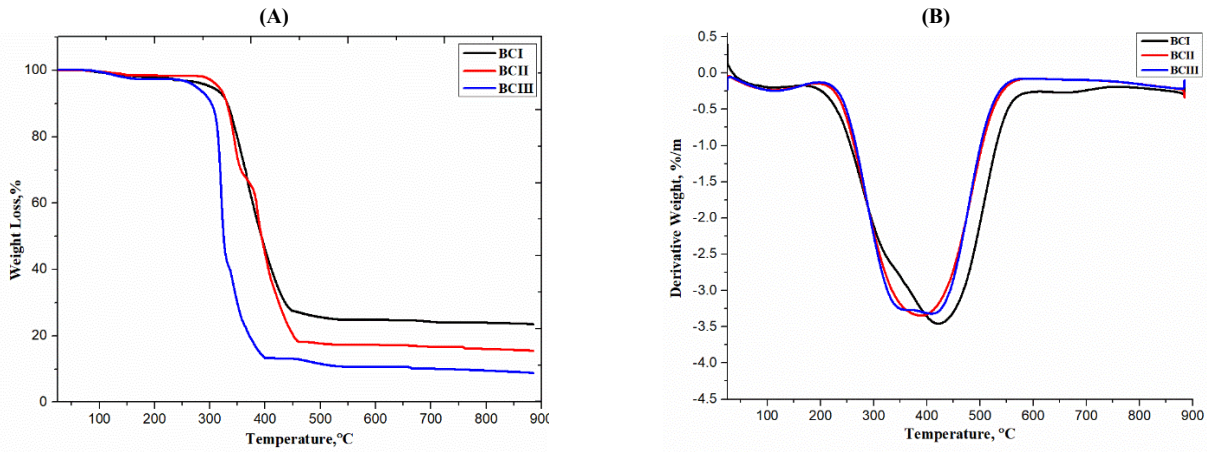

Fig. 4: TGA (A) and DTG (B) Curves of the Extracted Cellulose from Balanites Aegyptiaca Seed Shell.

The second and main degradation stage of the BCI, BCII, and BCIII cellulose samples occurred within the temperature ranges of 231.51-448.18°C, 280.70-462.94°C, and 237.84-403.72°C, respectively. The corresponding weight losses of 70.04%, 80.22%, and 84.14% suggest that the cellulose samples underwent almost complete combustion due to oxidative thermal degradation and destruction of the cellulose crystallite structure. The peak degradation temperatures in the second stage were observed at 423.38°C for BCI, 389.80°C for BCII, and 419.63°C for BCIII, as indicated by the DTG curve in Figure 4b. The thermal stability of the cellulose samples follows the sequence of decreasing residual weight: BCI > BCII > BCIII, with 23.46 wt.%, 15.47 wt.%, and 8.77 wt.%, respectively, at the highest temperature of 884°C. The higher weight residue in BCI and BCII may be attributed to the resistance of ash impurities to the alkaline and acidic bleaching treatments during the extraction and purification process.

4. Conclusion

Balanites aegyptiaca seed shells have been identified as a superior, previously untapped source of high-purity cellulose. This research demonstrates that the extracted fibers, particularly the BCI fraction, possess exceptional thermal stability and a high crystallinity index (up to 89.28%). The structural and morphological properties observed suggest that these fibers are ideal candidates for eco-friendly industrial applications, ranging from reinforced composites to bioactive cosmetic ingredients. By converting agricultural waste into high-value cellulose, this study provides a framework for the development of sustainable materials and encourages further optimization of biomass purification techniques.

Conflicts of Interest

The authors declare no conflict of interest.

Acknowledgements

Special appreciation goes to Prof. Uzama Danlami, Dr. Stella Adedunni Emmanuel, Mr. David Bwai Macham of the Chemistry Advanced Research Centre, Sheda Science and Technology Complex, Abuja, Nigeria, and Eng. Abdulrahaman Abdulhamid of the Central Laboratory of Umar Musa Yar'adua University, Katsina, Nigeria, for their support and patience.

Reference

[1] Naduparambath, S., Jinitha, T. V., Shaniba, V., Balan, S. M. P. A. K. and Purushothaman, E. (2018). Isolation and characterisation of cellulose nanocrystals from sago seed shells. *Carbohydrate Polymers*, *180*, 13–20. https://doi.org/10.1016/j.carbpol.2017.09.088.

[2] Fitriana, N. E., Suwanto, A., Jatmiko, T. H., Mursiti, S. and Prasetyo, D. J. (2020). Cellulose extraction from sugar palm (Arenga pinnata) fibre by alkaline and peroxide treatments. *IOP Conference Series: Earth and Environmental Science*, *462*(1). 1-6. https://doi.org/10.1088/1755-1315/462/1/012053.

[3] Johar, N., Ahmad, I. and Dufresne, A. (2012). Extraction, preparation and characterization of cellulose fibres and nanocrystals from rice husk. *Industrial Crops and Products*, *37*(1), 93–99. https://doi.org/10.1016/j.indcrop.2011.12.016.

[4] Liew, F. K., Hamdan, S., Rahman, M. R., Rusop, M., Lai, J. C. H., Hossen, M. F. and Rahman, M. M. (2015). Synthesis and characterization of cellulose from green bamboo by chemical treatment with mechanical process. *Journal of Chemistry*, *2015*: 212158. https://doi.org/10.1155/2015/212158.

[5] Frone, A. N., Chiulan, I., Panaitescu, D. M., Nicolae, C. A., Ghiurea, M. and Galan, A. M. (2017). Isolation of cellulose nanocrystals from plum seed shells, structural and morphological characterization. *Materials Letters*, *194*, 160–163. https://doi.org/10.1016/j.matlet.2017.02.051.

[6] Meireles, C. S., Filho, G. R., Fernandes, F. M., Cerqueira, D. A., Assunção, R. M. N., Ribeiro, E. A. M., Poletto, P. and Zeni, M. (2010). Characterization of asymmetric membranes of cellulose acetate from biomass: Newspaper and mango seed. *Carbohydrate Polymers*, *80*(3), 954–961. https://doi.org/10.1016/j.carbpol.2010.01.012.

[7] Ibrahim, M. M., Agblevor, F. A. andEl-Zawawy,W. K. (2010). Isolation and characterization of cellulose and lignin from steam-exploded lignocellulosic biomass. *BioResources*, *5*(1), 397–418. https://doi.org/10.15376/biores.5.1.397-418.

[8] Mansor, A. M., Lim, J. S., Ani, F. N., Hashim, H. and Ho, W. S. (2019). Characteristics of cellulose, hemicellulose and lignin of MD2 pineapple biomass. *Chemical Engineering Transactions*, *72*(December 2018), 79–84.

[9] Widiarto, S., Pramono, E., Suharso, Rochliadi, A. and Arcana, I. M. (2019). Cellulose nanofibers preparation from cassava peels via mechanical disruption. *Fibers*, *7*(5), 2–11. https://doi.org/10.3390/fib7050044.

[10] Trilokesh, C. and Uppuluri, K. B. (2019). Isolation and characterization of cellulose nanocrystals from jackfruit peel. *Scientific Reports*, *9*(1), 1–8. https://doi.org/10.1038/s41598-019-53412-x.

[11] Torgbo, S., Quan, V. M. and Sukyai, P. (2021). Cellulosic value-added products from sugarcane bagasse. *Cellulose*, *28*(9), 5219–5240. https://doi.org/10.1007/s10570-021-03918-3.

[12] Ranganagowda, R. P. G., Kamath, S. S. and Bennehalli, B. (2019). Extraction and Characterization of Cellulose from Natural Areca Fiber. *Material Science Research India*, *16*(1), 86–93. https://doi.org/10.13005/msri/160112.

[13] Altaher, A., Ahmed, O., Kita, A., Nemś, A., Miedzianka, J., Foligni, R., Mohamed, A., Abdalla, A and Mozzon, M. (2020). Tree - to - tree variability in fruits and kernels of a Balanites aegyptiaca (L .).Heidelberg. 34(1). 111-119. https://doi.org/10.1007/s00468-019-01901-x.

[14] Wakawa, A. I., Sambo, A. B. and Yusuf, S. (2018). *Phytochemistry and proximate composition of rootstem bark , leaf and fruit of desert date , Balanites aegyptiaca*. *7*(6), 464–470. https://doi.org/10.31254/phyto.2018.7602.

[15] Salam, S., Inoussa, C., Patrice, B., Firmin, S., Fréderic, S. B. and Mipro, H. (2025). Nutritional Value and Antinutritional Factors of Balanites aegyptiaca Seed Oils and Cakes for Animal Feed: A Review. *Food Science and Nutrition.* 13: e70478, 1-10. https://doi.org/10.1002/fsn3.70478.

[16] Diedhiou, D., Faye, M., Candy, L., Vandenbossche, V., Vilarem, G., Sock, O. and Rigal, L. (2021). *Composition and balance of the analytical fractionation of desert date (Balanites aegyptiaca L .) seeds harvested in Senegal*. *20*(4), 150–158.

[17] Rajanna, M. Shivashankar, L. M. Shivamurthy, O. H. Ramachandrappa, S. U.; Betageri, V. S. Shivamallu, C.Shetty, R. H. L. Kumar, S. Amachawadi, R.G. Kollur, S. P. (2022). A Facile Synthesis of Cellulose Nanofibers from Corn Cob and Rice Straw by Acid Hydrolysis Method. Polymers 2022, 14, 4383. https://doi.org/10.3390/ polym14204383.

[18] Ogunjobi, J. K. and Balogun, O. M. (2021). Isolation, modification and characterisation of cellulose from wild Dioscorea bulbifera. *Scientific Reports*, *11*(1), 1–10. https://doi.org/10.1038/s41598-020-78533-6.

[19] Arar, Ö. (2019). Preparation of anion-exchange cellulose for the removal of chromate. *Journal of the Chilean Chemical Society*, *64*(2), 4471–4474. https://doi.org/10.4067/S0717-97072019000204471.

[20] Mohd Jamil, N. A., Jaffar, S. S., Saallah, S., Misson, M., Siddiquee, S., Roslan, J. and Enggoro, W.(2022).Isolation of Cellulose Nanocrystals from Banana Peel Using One-Pot Microwave and Mild Oxidative Hydrolysis System. Nanomaterials 2022, 12, 3537. https://doi.org/10.4067/S0717-97072019000204471.

[21] Md Salim, R., Asik, J., and Sarjadi, S. M. (2021). Chemical functional groups of extractives, cellulose and lignin extracted from native *Leucaena leucocephala* bark. Wood Science and Technology. 55:295–313. https://doi.org/10.1007/s00226-020-01258-2.

[22] Mugesh, S., Kumar, P. T. andMurugan, M. (2016). An unprecedented bacterial cellulosic material for defluoridation of water. Royal Society of Chemistry Advances. 6, 104839–104846. https://doi.org/10.1039/C6RA22324A.

[23] Coates, J. (2000). *Interpretation of Infrared Spectra , A Practical Approach*. 10815–10837. https://doi.org/10.1002/9780470027318.a5606.

[24] Ogunjobi, K. J., Adewale, I. A. and Adeyemi, A. S. (2023). Cellulose nanocrystals from Siam weed: Synthesis and physicochemical characterization. Heliyon 9 (2023) e13104. https://doi.org/10.1016/j.heliyon.2023.e13104.

[25] Romruen, O., Karbowiak, T, Tongdeesoontorn, W., Shiekh, K. A. and Rawdkuen S. (2022). Extraction and Characterization of Cellulose from Agricultural By-Products of Chiang Rai Province, Thailand. Polymers 2022, 14, 1830. https://doi.org/10.3390/polym14091830.

[26] Cheran, E., Rahale, S. C., Lakshmanan, A., Subramanian, P., Raja, K. and Divyabharathi, P. (2022). Synthesis and Characterization of a Novel Maize Cob Based Nanocellulose. *International Journal of Plant & Soil Science.* 34(21): 678-687. https://doi.org/10.9734/ijpss/2022/v34i2131318.

[27] Mishra, D., Khare, P., Das, R. M., Mohanty, S., Kule, B. U. D. and Kumar, A. V. P. (2018). Characterization of Crystalline Cellulose Extracted from Distilled Waste of Cymbopogon Winterianus. *Cellulose Chemistry and Technology.* 52 (9-2), 9-17.

[28] Zambrano-Mite, F. L., Villasana, Y., Bejarano, L. M., Luciani, C., Niebieskikwiat, D., Alvarez, W., Cueva, F. D., Aguilera-Pesantes, D. and Lourdes M. Orejuela-Escobar, M. L. (2023). Optimization of microfibrillated cellulose isolation from cocoa pod husk via mild oxalic acid hydrolysis: A response surface methodology approach. Heliyon 9, 1-12. www.cell.com/heliyon. https://doi.org/10.1016/j.heliyon.2023.e17258.

[29] Khan, N. M., Ahmad, A., Rehman, N., Kelestemur, S., Tariq, M., Jan, A. K., Ahmad, S., Eisele, M. D., Syed, W. and Al-Rawi, A. B. M. (2025). Extraction and characterization of cellulose and cellulose nanocrystals from the stalks of Marrubium vulgare plant. *Carbohydrate Polymer Technologies and Applications.* 11,1-7. https://doi.org/10.1016/j.carpta.2025.100947.

[30] Oun, A. A. and Rhim, J. (2018). Isolation of oxidized nanocellulose from rice straw using the ammonium persulfate method. *Cellulose*. 25, 2143–2149. https://doi.org/10.1007/s10570-018-1730-6.

[31] Huntley, C. J., Crews, K. D., Abdalla, M. A., Russell, A. E., & Curry, M. L. (2015). Influence of strong acid hydrolysis processing on the thermal stability and crystallinity of cellulose isolated from wheat straw. International Journal of Chemical Engineering, 2015. https://doi.org/10.1155/2015/658163.

[32] Mesoppirr, L. S., Suter, E. K., Omwoyo, W. N., Oyaro, N. M. and Nelana, S. M. (2024) Isolative Synthesis and Characterization of Cellulose and Cellulose Nanocrystals from Typha angustifolia. Open Journal of Applied Sciences, 14, 2443-2459. https://doi.org/10.4236/ojapps.2024.149161.

[33] Sathishkumar, P., Shah, A. M., Panchal, H., Sharma, K., Gopinath, R., Sanjay, M. R., Siengchin, S., Kumar, R. L. and Rampradheep, G. S. (2024). Characterization of new cellulose fiber extracted from second generation Bitter Albizia tree T. Scientific Reports. 14:1693. https://doi.org/10.1038/s41598-024-51719-y.

[34] Khenblouche, A., Bechki, D., Gouamid, M., Charradi, K., Segni, L., Hadjadj, M., and Boughali, S. (2019). Extraction and characterization of cellulose microfibers from Retama raetam stems. *Polímeros: Ciência e Tecnologia*, *29*(1), e2019011. https://doi.org/10.1590/0104-1428.05218.

[35] Lee, C. Y., Mat, U. W. and Norhayani, O. (2015). Thermal and Flexural Properties of Regenerated Cellulose(Rc)/Poly(3-Hydroxybutyrate)(Phb)Biocomposites. Jurnal Teknologi (Sciences and Engineering) 75:11 (2015) 107–112. https://doi.org/10.11113/jt.v75.5338.